Bioconjugate Chemistry

Article

pubs.acs.org/bc

Continuous Monitoring of Enzymatic Reactions on Surfaces by Real-Time Flow Cytometry: Sortase A Catalyzed Protein Immobilization as a Case Study

Tobias Heck,[†] Phu-Huy Pham,[†] Frederik Hammes,[‡] Linda Thöny-Meyer,[†] and Michael Richter*[,†]

[†]Laboratory for Bioactive Materials, Empa, Swiss Federal Laboratories for Materials Science and Technology, Lerchenfeldstrasse 5, 9014 St. Gallen, Switzerland

[‡]Department of Environmental Microbiology, Eawag, Swiss Federal Institute of Aquatic Science and Technology, Überlandstrasse 133, 8600 Dübendorf, Switzerland

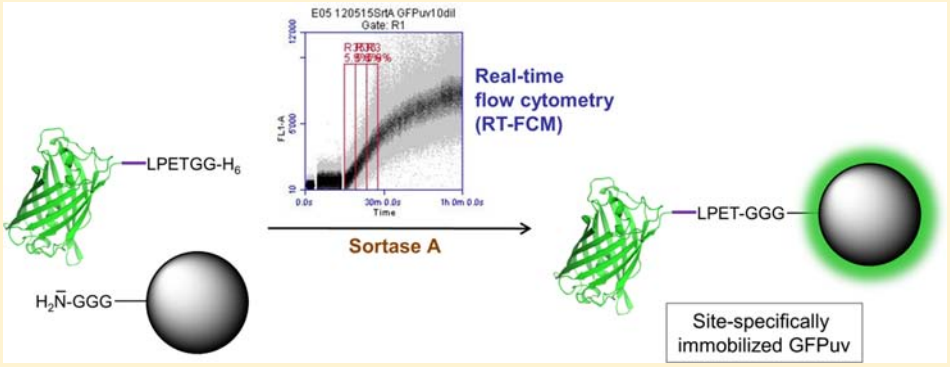

ABSTRACT: Only a few techniques, such as quartz crystal microbalance and surface plasmon resonance spectroscopy, enable the analysis of dynamic processes on solid supports. Here we have developed a straightforward assay based on flow cytometry to continuously follow enzymatic reactions directly on microparticle surfaces. We applied this real-time flow cytometry (RT-FCM) approach to study the covalent immobilization of green-fluorescent protein (GFPuv) on triglycine-modified polystyrene microbeads by the transpeptidase sortase A (SrtA) from *Staphylococcus aureus*. Though commonly treated as functionally identical catalysts, the SrtA variants $SrtA_{\Delta 59}$ and $SrtA_{\Delta 25}$, in which the N-terminal amino acid residues 1−59 and 1−25 of the native enzyme are truncated, were shown to perform very differently with regard to this particular immobilization reaction. While $SrtA_{\Delta 59}$ efficiently catalyzed the covalent attachment of GFPuv to the surface (as indicated by a linear increase of microbead fluorescence), $SrtA_{\Delta 25}$ was essentially inactive. Besides the length of the N-terminal amino acid extension on the SrtA construct, the position of the hexahistidine tag at either the N- or C-terminus affected the efficiency of enzymatic protein immobilization. Apart from three enzyme variants containing the native core structure of SrtA, we also included three recently evolved mutants of SrtA in this comparative study. With these mutants we observed a rapid initial attachment of the GFPuv target protein to the microbeads. However, with proceeding reaction time, cleavage of the covalently immobilized target protein from the surface prevailed over the coupling reaction, consequently causing a decline of microbead fluorescence. In general, the RT-FCM approach used herein represents a powerful analytical tool for qualitative dynamic studies of many heterogeneous enzymatic reactions or other binding events that influence the fluorescence properties of microparticle surfaces.

INTRODUCTION

The immobilization of functional proteins and enzymes on solid matrices is of considerable importance in many areas of application, such as industrial biocatalysis,[1−3] medical diagnostics,[4,5] and environmental monitoring.[6,7] Depending on the intended purpose of use, the strategy for surface immobilization of the protein needs to be carefully considered, as it represents a major factor that determines the specifications of the fabricated hybrid material. Comprehensive review articles summarizing the commonly used immobilization techniques have been published recently by Wong et al. and Redeker et al.[8,9] Most conventional approaches rely on nonspecific physical adsorption of the protein to the carrier material by hydrophobic or ionic interactions, or on chemical reactions of functional amino acid side chains with reactive moieties at the surface. Despite the benefit of simplicity, these nonspecific methodologies usually generate undefined, inhomogeneous layers of proteins in random orientation, which often compromises the functionality of the immobilized protein due to unfolding and denaturation, steric inaccessibility of the substrate-binding region, or hindered diffusion of substrates to the active site. The issue of protein orientation at the surface can be solved by

Received: May 22, 2014
Revised: July 14, 2014
Published: July 30, 2014

   dx.doi.org/10.1021/bc500230r | *Bioconjugate Chem.* 2014, 25, 1492−1500

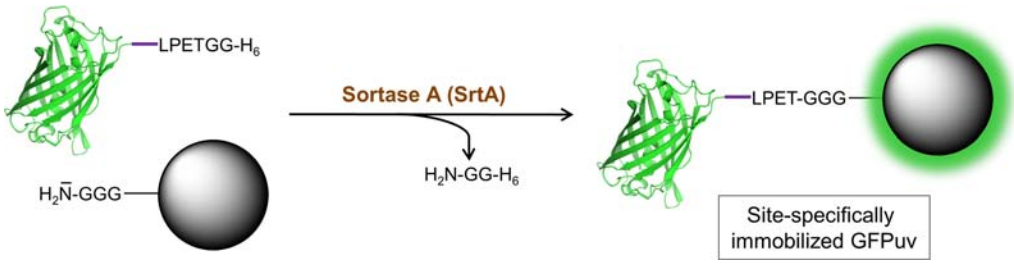

Figure 1. Schematic representation of SrtA-catalyzed GFPuv immobilization on triglycine functionalized polystyrene microbeads. A flexible linker (GGGGS; purple) has been introduced between the GFPuv core and the LPETG sorting motif in order to reduce intermolecular cross-linking reactions between GFPuv molecules.[29]

fusing the protein to affinity tags (e.g., polyhistidine, FLAG, or calmodulin tag) that selectively confer protein adsorption to specifically tailored complementary surfaces in a defined orientation.[10] Due to the noncovalent nature of these binding interactions, leaching of the protein from the support may occur and thus affect the lifetime of the protein hybrid material. As an alternative to noncovalent immobilization approaches, bioorthogonal chemoligation strategies have attracted increasing attention because they facilitate the site-specific and covalent immobilization of proteins under mild reaction conditions.[11] These methods generally require a process of two sequential steps, namely, (i) labeling of the target protein with a unique reactive group that is not found in the natural amino acids and (ii) the actual immobilization reaction to anchor the previously functionalized protein on the appropriate carrier material. For this purpose, an azide group is most commonly introduced at a specific site of the protein that may then react with an activated phosphine moiety (Staudinger ligation) or an alkyne component (1,3-dipolar cycloaddition, colloquially known as "click" reaction) exposed on the surface.

Apart from chemical immobilization strategies, enzymatic approaches mediating the covalent attachment of proteins on solid supports in an oriented fashion are frequently employed. Examples of enzymes that have been shown to catalyze reactions directly between a protein of interest and a surface include microbial transglutaminase (MTG) from *Streptomyces mobaraensis*,[12] phosphopantetheine transferase (PPTase),[13] and the transpeptidase sortase A (SrtA) from *Staphylococcus aureus*.[14] In the present report, we focused on the use of SrtA because this enzyme has already been applied for the immobilization of various target proteins tagged with a SrtA-specific LPXTG amino acid motif on different types of solid supports functionalized with an oligoglycine acceptor moiety. Examples include the immobilization of fluorescent proteins on polymer microbeads and liposomes,[15−18] human and bacterial glycosyltransferases on sepharose particles,[19] single-chain variable antibody fragments on PEGylated polymer capsules,[20] fibronectin binding protein on CM5 biosensor chips,[21] and recombinant human thrombomodulin on glass slides.[22]

Due to the limited number of techniques that enable continuous monitoring of protein attachment on surfaces (e.g., quartz crystal microbalance (QCM)[23,24] and surface plasmon resonance spectroscopy (SPR)[25,26]), the efficiency of immobilization reactions is usually judged by end point assays evaluating functional properties of the obtained protein hybrid material, such as fluorescence intensity, enzymatic activity, or binding affinity.[12,13,15−22] This generally complicates the optimization of enzyme-catalyzed immobilization reactions and leads to the fact that process parameters such as concentration of enzyme and reactants, buffer conditions, temperature, and reaction time are in most cases chosen empirically. In the case of immobilization reactions catalyzed by SrtA, another important, yet mostly neglected factor, is the choice of the enzyme variant employed for the particular coupling reaction. Though all constructs of SrtA used for the above-mentioned immobilization scenarios share identical catalytic core structures, they comprise variations in (i) the length of the N-terminal amino acid stretch derived from the membrane-anchoring domain of full-length SrtA and (ii) the type and location of the affinity tag added for straightforward purification of the enzyme. Evaluating the use of SrtA enzymes for transpeptidation reactions between two soluble target proteins, we recently demonstrated that the N-terminally His-tagged variants H_6-$SrtA_{\Delta 59}$ (truncation of amino acid residues 1−59) and H_6-$SrtA_{\Delta 25}$ (truncation of amino acid residues 1−25), which have been previously described as functionally identical enzymes,[27,28] and various evolved mutants of a C-terminally His-tagged $SrtA_{\Delta 59}$-H_6 variant have very different coupling properties.[29]

In the present study, we established a continuous assay to investigate the dynamics of heterologous enzymatic reactions at particle surfaces in real time. Our concept is based on the consideration of elapsed measurement time as an additional analytical parameter in classical flow cytometry experiments.[30,31] The temporal resolution of individual data points expands the application spectrum of flow cytometry from static analyses of cell and particle populations in equilibrium state[32] to dynamic studies of various biological and biochemical processes. Using this so-called kinetic or real-time flow cytometry (RT-FCM) approach, reactions in biotic systems, such as stimuli-induced changes of calcium concentrations in mammalian cells[33,34] and stress responses of microorganisms to environmental changes,[35] as well as kinetic analyses of abiotic systems, such as ligand−receptor interactions[36,37] and mechanistic enzyme studies using surface-bound substrates,[38,39] have been investigated. Herein, we adapted the RT-FCM approach established by Arnoldini and co-workers[35] to continuously follow the covalent immobilization of green-fluorescent protein (GFPuv) by six catalytically diverse variants of the enzyme SrtA (Figure 1).[29] The efficiency of GFPuv immobilization by the SrtA variants could be deduced from the dynamic change of microbead fluorescence monitored over time by RT-FCM. Apart from the qualitative comparison of the studied enzyme variants, the impact of substances affecting the enzymatic immobilization reaction (e.g., enzyme inhibitors) could be easily assessed in real time immediately after addition of the particular compound.

dx.doi.org/10.1021/bc500230r | *Bioconjugate Chem.* 2014, 25, 1492−1500

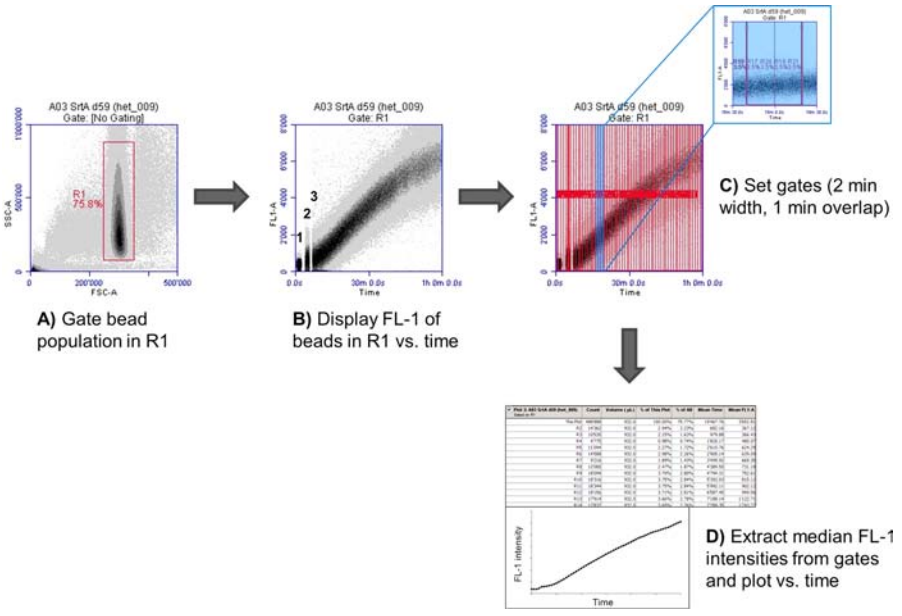

Figure 2. Overview of RT-FCM acquisition and data evaluation. Each data point displayed on the density plots represents one single particle event detected by the flow cytometer. FSC: forward scatter, indicative of particle size; SSC: sideward scatter, indicative of particle composition; FL-1: green fluorescence intensity. Gate R1 represents the population of microbeads (A) and is used as the primary selector for subsequently performed real-time experiments. Real-time data acquisition (B) is started with a sample of microbeads suspended in reaction buffer (step 1) to which the LPETG-tagged GFPuv target protein (step 2) and the SrtA catalyst (step 3) are sequentially added at intervals of 2 min. For data analysis, the particle events recorded over the reaction period are binned in 2-min-wide overlapping gates (C), from which the median FL-1 intensities are extracted and graphically displayed (D).

RESULTS AND DISCUSSION

RT-FCM Setup for Determination of SrtA Activity on Microparticle Surfaces. Flow cytometry is a powerful technique routinely used for qualitative and quantitative analyses of living cells in the fields of biomedical research,[32] microbiology,[40] and biotechnology.[41,42] In a classical flow cytometry experiment, information about the relative size, granularity, and fluorescence emission characteristics of each individual cell passing the laser beam is acquired. The cumulative data obtained for a measured sample reflects the properties of the cell population at the particular time of analysis. In addition to the measured standard parameters, RT-FCM considers time as an additional parameter in flow cytometry and therefore paves the way for real-time analysis of cellular populations. In short, with RT-FCM a sample is continuously assessed during minutes to hours without interruption, and dynamic changes in the sample suspension are tracked by binning the acquired data at selected time intervals.

In the present study, we adapted the RT-FCM approach established by Arnoldini and co-workers for dynamic studies of microbial populations[35] to investigate the kinetics of heterogeneous enzymatic reactions at microparticle surfaces. Our reaction of interest was the SrtA-catalyzed covalent immobilization of LPETG-tagged green fluorescent protein (GFPuv) on triglycine-functionalized polystyrene microbeads; a schematic representation of this transpeptidation reaction is presented in Figure 1. The enzymatic reaction was routinely carried out in an open 1.5 mL polypropylene reaction vessel with the sample injection port of the flow cytometer directly submerged in the reaction suspension. In this setup, the sample was continuously fed to the flow cytometer at a constant flow rate while the enzymatic reaction in the reaction vessel proceeded, thus avoiding time-consuming and error-prone individual sampling and analysis steps. Each microbead particle passing the laser beam was recorded by the instrument as a single "event" that could be displayed in 2D density plots based on the detected parameters FSC (forward scattered light, indicative of particle size), SSC (sideward scattered light, indicative of particle composition), and/or fluorescence intensity. In the reaction scenario investigated here, RT-FCM was applied to monitor the increase of green fluorescence intensity (FL-1) of the microbead population with time, reflecting the progress of the SrtA-catalyzed covalent attachment of GFPuv molecules to the particle surface.

The standard procedure followed for acquisition and processing of SrtA kinetic data is depicted in Figure 2. Prior to each set of real-time experiments, a blank microbead sample was processed, and the population of microbeads was localized on a scatter plot (FSC vs SSC) and gated (Figure 2A). This gate (R1) served as the primary selector to separate the main signal of interest (i.e., fluorescence intensity of the microbeads) from background events recorded. During real-time data acquisition the fluorescence intensity of each microbead event detected within the borders of gate R1 was monitored and concurrently displayed over time on a density plot (Figure 2B). As a consequence of using an open reaction vessel, reactants could easily be added to the reaction mixture in a stepwise manner, and their impact on the fluorescence characteristics of the microbead population could be monitored continuously while uninterrupted data acquisition proceeded. Routinely, each real-time analysis was initiated with the acquisition of the untreated microbead suspension in order to identify the background fluorescence signal generated by the unmodified microbead population (Figure 2B, step 1). After an acquisition time of 2 min the GFPuv target protein was added to the reaction mixture, causing a shift of microbead fluorescence to higher signal intensity due to spontaneous adsorption of

dx.doi.org/10.1021/bc500230r | Bioconjugate Chem. 2014, 25, 1492−1500

Table 1. Summary of SrtA-Catalyzed (i) GFPuv Immobilization on Triglycine-Modified Polystyrene Microbeads and (ii) GFPuv-F_M Transpeptidation in Solution

SrtA variant			immobilization of GFPuv-linker-LPETGG-H_6 on GGG-polystyrene beads		transpeptidation between GFPuv-linker-LPETGG-H_6 and GGG-H_6-F_M
acronym	structural features	reference	apparent initial rate (change of FL-1 per min)[a]	max. FL-1 intensity of beads[b]	apparent initial rate (change of product band intensity per min)[c]
H_6-$SrtA_{\Delta 59}$	Amino acids 1−59 deleted; N-terminal hexahistidine tag	Heck et al.[29]	129	6359	0.39
H_6-$SrtA_{\Delta 25}$	Amino acids 1−25 deleted; N-terminal hexahistidine tag	Duong et al.[57]	3.2	657	0.18
$SrtA_{\Delta 59}$-H_6	Amino acids 1−59 deleted; C-terminal hexahistidine tag	Chen et al.[46]	22	1511	0.38
^{3}*$SrtA_{\Delta 59}$-H_6	Triple mutant of $SrtA_{\Delta 59}$-H_6 (P94S, D160N, D165A)	Chen et al.[46]	94	1858	8.2
^{4}*$SrtA_{\Delta 59}$-H_6	Tetra mutant of $SrtA_{\Delta 59}$-H_6 (P94S, D160N, D165A, K196T)	Chen et al.[46]	208	1968	8.8
^{5}*$SrtA_{\Delta 59}$-H_6	Penta mutant of $SrtA_{\Delta 59}$-H_6 (P94R, D160N, D165A, K190T, K196T)	Chen et al.[46]	364	2721	11

[a]The apparent rate values were calculated from the initial slopes of the progress curves depicted in Figure 5A. [b]In the case of reactions catalyzed by H_6-$SrtA_{\Delta 59}$, H_6-$SrtA_{\Delta 25}$, and $SrtA_{\Delta 59}$-H_6 no saturation of FL-1 intensity was reached over the reaction period of 1 h; thus, the given values correspond to the FL-1 intensities of the microbead populations after completion of the enzymatic reactions. In the case of reactions catalyzed by the mutants ^{3}*$SrtA_{\Delta 59}$-H_6, ^{4}*$SrtA_{\Delta 59}$-H_6, and ^{5}*$SrtA_{\Delta 59}$-H_6 the given values correspond to the maximum FL-1 intensities reached before microbead fluorescence slowly faded due to subsequent enzymatic side reactions. [c]The apparent rate values were calculated from the initial slopes of the progress curves depicted in Figure 5B.[29]

fluorescent protein molecules to the polystyrene surface (Figure 2B, step 2). After equilibration of the system for an additional 2 min, the enzymatic reaction was started by the addition of SrtA and the enzyme-catalyzed immobilization reaction was followed by monitoring the time-dependent change of microbead fluorescence due to covalent attachment of GFPuv (Figure 2B, step 3). The acquired microbead events—each bead represented by one data point on the time vs FL-1 plot—were further processed by binning the data in 2-min-wide overlapping gates (Figure 2C), followed by extraction and graphical display of the median fluorescence intensity values obtained for each gate (Figure 2D).

Reaction Dynamics and Inhibition of GFPuv Immobilization Catalyzed by SrtA. The transpeptidation activity of SrtA enzymes is commonly determined in solution using a small LPETG-containing peptide substrate labeled with a fluorophore−quencher pair (Dabcyl/Edans or Abz/Dnp) in the presence of an oligoglycine acceptor peptide. Analysis of the catalytic reaction is then performed either continuously by fluorescence spectroscopy[28,43−45] or discontinuously by high-performance liquid chromatography (HPLC).[46−48] However, due to inconsistent values obtained for the kinetic parameters of the SrtA-catalyzed coupling reaction, the use of these two techniques has been controversially discussed.[47]

Here we applied the RT-FCM approach described in the previous section for the qualitative analysis of GFPuv immobilization on triglycine-functionalized polystyrene microbeads catalyzed by six SrtA variants (Table 1) under varying reaction conditions. For the coupling reactions we routinely employed the target protein variant GFPuv-linker-LPETGG-H_6; the linker inserted between the GFPuv core and the LPETG sorting motif is composed of five amino acids (GGGGS) and has been shown to minimize unspecific cross-link formation between GFPuv monomers.[29]

Under the standard assay conditions the fluorescence intensity of the microbead population increased steadily after the addition of H_6-$SrtA_{\Delta 59}$ (Figure 2B and Figure 3A). At the employed enzyme concentration of 2 μM, no saturation of bead fluorescence was reached after 1 h, indicating that GFPuv immobilization still proceeded at the end of the monitored reaction period. The apparent initial rate of the immobilization reaction (measured as the increase of FL-1 intensity per minute) was linearly dependent on the added concentration of GFPuv-linker-LPETGG-H_6 (Figure 3A, cf. curves at target protein concentrations of 0.5 μM and 0.1 μM). When $CaCl_2$ was omitted from the reaction mixture or GFPuv-linker-LAETGG-H_6 was used instead of GFPuv-linker-LPETGG-H_6, no significant increase of fluorescence intensity was detected over the monitored reaction period, suggesting that no or only negligible covalent GFPuv attachment to the microbead surface occurred under these conditions (Figure 3A). These results demonstrate (i) the calcium dependence of the enzyme and (ii) the selectivity of the H_6-$SrtA_{\Delta 59}$-catalyzed immobilization reaction for target proteins carrying the correct LPETG sorting motif. The use of commercially available alkyl-amino terminated polystyrene beads instead of the routinely employed triglycine-functionalized microbeads led to increased non-specific protein adsorption to the material as indicated by an immediate increase of the fluorescence signal after addition of the GFPuv target protein (Figure 3A). After addition of SrtA, a slow continuous rise of microbead fluorescence was observed over the reaction period of 1 h, suggesting a weak immobilization activity of SrtA on the alkyl-amino polystyrene surface. Likewise, a low level of SrtA-catalyzed GFPuv immobilization on alkyl-amino microbeads was observed when the reactions were run at increased concentrations of reactants under vigorous shaking and analyzed by fluorescence microscopy (Figure 4). This result is in agreement with SrtA-catalyzed transpeptidation experiments in solution, revealing that besides terminal oligoglycine moieties also alkyl-amino side chains of lysine residues may act as nucleophiles to generate isopeptide bond cross-links between the target proteins.[29,49]

Figure 3B depicts the progress of the SrtA-catalyzed immobilization reaction when ethylenediaminetetraacetate (EDTA) or free triglycine peptide were added as inhibitors to the reaction mixture. The soluble triglycine peptide competes with the triglycine-functionalized microbead surface for the SrtA-GFPuv acyl enzyme intermediate in a concen-

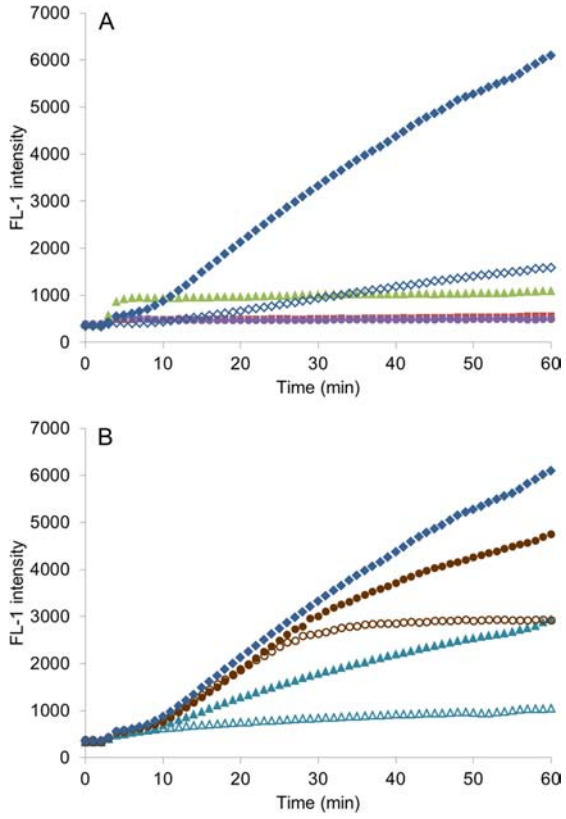

Figure 3. SrtA-catalyzed GFPuv immobilization on polystyrene microbeads as monitored by RT-FCM. The reaction under standard assay conditions (2 μM H_6-$SrtA_{\Delta 59}$, 0.5 μM GFPuv-linker-LPETGG-H_6, 0.9 × 10^6 triglycine-modified beads per mL in 50 mM Tris-HCl buffer pH 7.8, 150 mM NaCl, 10 mM $CaCl_2$) is displayed as blue diamonds in both graphs. Each data point represents the mean value of three independently conducted experiments. Standard deviations for each data point ranged below 10%. (A) Filled and open blue diamonds represent reactions run at 0.5 μM and 0.1 μM GFPuv-linker-LPETGG-H_6, respectively. Negligible enzymatic immobilization of GFPuv was observed in reactions run with nonmodified alkyl-amino polystyrene beads (green triangles), without addition of $CaCl_2$ (purple circles), or with the altered target protein GFPuv-linker-LAETGG-H_6 (red squares). (B) Inhibition of GFPuv immobilization by (i) EDTA added after 24 min to running reactions at concentrations of 1.5 mM (filled brown circles) and 15 mM (open brown circles) or (ii) free triglycine peptide added to the initial reaction mixtures at concentrations of 0.5 mM (filled turquoise triangles) and 10 mM (open turquoise triangles).

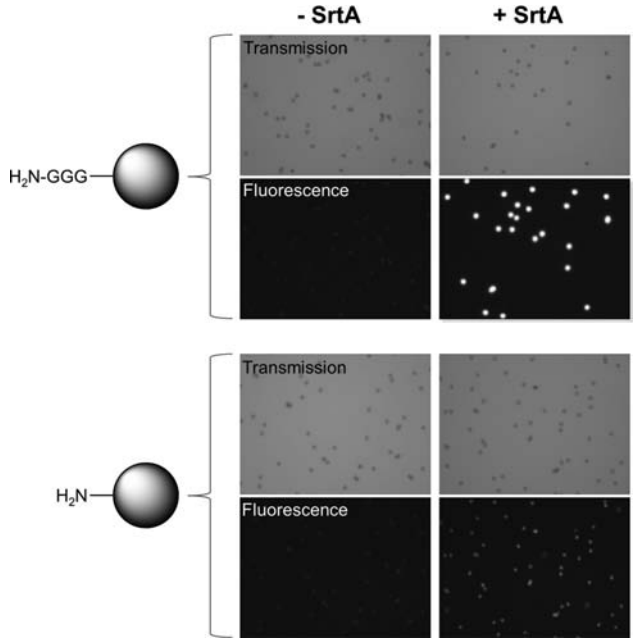

Figure 4. SrtA-catalyzed immobilization of LPETG-tagged GFPuv on 3 μm triglycine-modified polystyrene beads (top) and alkyl-amino terminated polystyrene microbeads (bottom). After the coupling reaction bead samples were rigorously washed to remove non-covalently bound protein from the beads. For each sample a transmission microscopy image and a fluorescence image is shown.

tration-dependent manner, thus reducing the velocity of the enzyme-catalyzed immobilization reaction. In contrast, EDTA is known to deactivate SrtA by chelating the Ca^{2+} ion required for activity of the enzyme.[16,28,44] When EDTA was added at a concentration of 1.5 mM to a running reaction batch the enzyme remained partially active, whereas the addition of 15 mM EDTA completely interrupted GFPuv immobilization on the microbeads by SrtA. Finally, it should be mentioned that the reaction curves of GFPuv immobilization depicted in Figure 3 and Figure 5A were highly reproducible; standard deviations below 10% were obtained for each data point extracted from three independently measured sets of RT-FCM raw data. However, long-term storage of a buffered suspension of triglycine-functionalized polystyrene microbeads over a period of several months altered the material properties of the particles. This change was evident from a drastically retarded immobilization of GFPuv by SrtA as compared to control reactions performed on the same day with a freshly functionalized batch of particles (results not shown).

Reaction Dynamics of GFPuv Immobilization by Different SrtA Variants. We have recently compared the catalytic properties of six SrtA variants from *S. aureus* with regard to site-specific transpeptidation and competing intermolecular cross-linking reactions between two protein species in solution;[29] the critical structural features of the studied SrtA enzymes are summarized in Table 1. As an example from our previous study, reaction curves showing the time-dependent formation of the heterodimeric transpeptidation product GFPuv-F_M from the donor protein GFPuv-linker-LPETGG-H_6 and the acceptor protein GGG-H_6-F_M by the six tested SrtA variants are depicted in Figure 5B. All six SrtA variants catalyzed the formation of the desired product as well as competing isopeptide-bond cross-linking and hydrolysis reactions with the GFPuv target protein at different apparent catalytic rates.[29] Using the RT-FCM approach, we investigated the properties of the same six SrtA enzymes when employed as catalysts for the site-specific immobilization of the target protein GFPuv-linker-LPETGG-H_6 on triglycine-functionalized polystyrene microbeads (see Figure 1); the progress curves of the immobilization reactions catalyzed by the different SrtA variants as measured by the time-dependent increase of microbead fluorescence intensity are depicted in Figure 5A. As we focused on the qualitative comparison of the enzymes, the quantification of surface-bound fluorophores by fluorescence calibration[39,50−52] and the subsequent deduction of kinetic parameters describing the enzymatic surface reactions[53,54] were not a matter of the present study. These issues have been addressed and discussed in detail for other reaction systems in the specified publications.

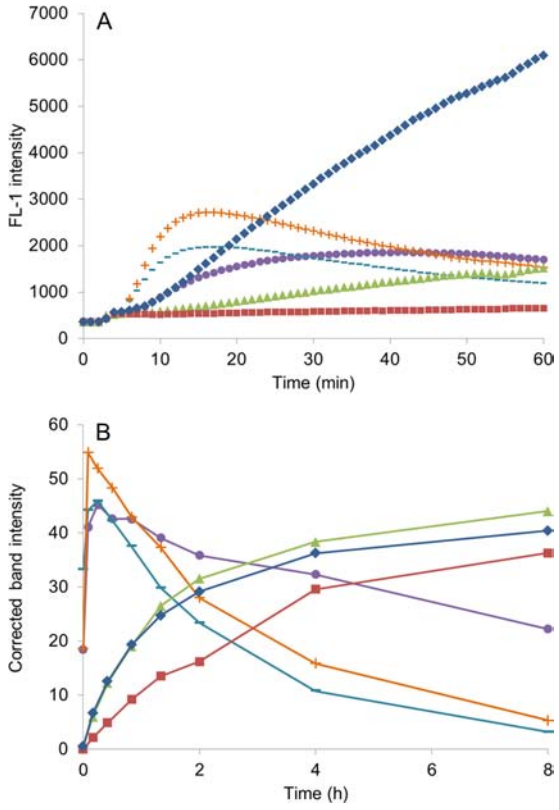

Figure 5. Comparison of coupling reactions catalyzed by six variants of SrtA. The SrtA variants H_6-$SrtA_{\Delta 59}$ (blue diamonds), H_6-$SrtA_{\Delta 25}$ (red squares), $SrtA_{\Delta 59}$-H_6 (green triangles), ^{3}*$SrtA_{\Delta 59}$-H_6 (purple circles), ^{4}*$SrtA_{\Delta 59}$-H_6 (turquoise dashes), and ^{5}*$SrtA_{\Delta 59}$-H_6 (orange crosses) were used at a concentration of 2 μM. (A) SrtA-catalyzed immobilization of GFPuv-linker-LPETGG-H_6 (0.5 μM) on triglycine-functionalized polystyrene beads (3 μm; 0.9×10^6 beads per mL) as monitored by RT-FCM. Each data point represents the mean value of three independently conducted experiments. Standard deviations for each data point ranged below 10%. (B) SrtA-catalyzed covalent fusion of GFPuv-linker-LPETGG-H_6 (10 μM) to the acceptor protein GGG-H_6–F_M (10 μM), a variant of the human FK 12-binding protein. The graphs show the formation of the heterodimeric transpeptidation product as determined by image analysis of SDS-PAGE gels in a previous study.[29]

In this section, we contrast the results of the present study focusing on SrtA-catalyzed reactions of a soluble donor target protein with a solid acceptor surface (Figure 5A and Table 1) with results previously obtained for SrtA-catalyzed reactions involving a donor protein and an acceptor protein in solution (Figure 5B).[29] While the location of the hexahistidine tag on either the N- or the C-terminus of the SrtA construct did not affect the transpeptidation reaction in solution, H_6-$SrtA_{\Delta 59}$ catalyzed the immobilization of the GFPuv target protein on the microbead surface with an approximately 6-fold higher apparent reaction rate than the C-terminally His-tagged variant $SrtA_{\Delta 59}$-H_6 (cf. Figure 5A,B, Table 1). With the enzyme H_6-$SrtA_{\Delta 59}$, which carries an extension of approximately 40 amino acids between the N-terminal hexahistidine tag and the enzymatic core, transpeptidation in solution occurred at only slightly reduced apparent rates compared to reactions using the fully truncated variant H_6-$SrtA_{\Delta 59}$. Interestingly, when we used the same H_6-$SrtA_{\Delta 25}$ variant in the present heterogeneous reaction system, only negligible immobilization of the GFPuv target protein on the microbead surface was detected. We assume that the additional amino acid stretch within H_6-$SrtA_{\Delta 25}$, which is derived from the membrane anchor of the native enzyme, either hinders access of the surface-attached triglycine acceptor peptide to the active site of the enzyme or leads to adsorption and potential subsequent denaturation of H_6-$SrtA_{\Delta 25}$ at the polystyrene surface. In contrast to our finding, other investigations using the same partially truncated H_6-$SrtA_{\Delta 25}$ variant revealed successful protein immobilization on modified glass slides, polymer beads and capsules as determined by functional analysis of the final product.[15,20] In both of these studies, long spacers had been introduced between the surface and the surface-bound oligoglycine peptide, conferring additional flexibility for the interaction between enzyme and substrate. This supports our hypothesis that most likely steric restrictions limit immobilization reactions catalyzed by H_6-$SrtA_{\Delta 25}$ to solid acceptor substrates having a certain degree of conformational flexibility.

Employing three recently discovered mutants of SrtA[46] for transpeptidation reactions in solution, the heterodimeric GFPuv-F_M product was formed at much higher apparent initial rates than with the respective wild-type variant $SrtA_{\Delta 59}$-H_6 (Figure 5B).[29] However, with the mutated enzymes the transpeptidation product accumulated to a maximum before it underwent subsequent enzyme-catalyzed hydrolysis and intermolecular cross-linking reactions. Similar reaction courses were monitored with the RT-FCM approach when analyzing the immobilization of GFPuv-linker-LPETGG-H_6 to the triglycine-functionalized microbeads by the tetra mutant ^{4}*$SrtA_{\Delta 59}$-H_6 and the penta mutant ^{5}*$SrtA_{\Delta 59}$-H_6 (Figure 5A). After the initial rapid attachment of the GFPuv target protein to the microbead surface the acquired level of particle fluorescence slowly faded with advancing reaction time. This can likely be explained by the fact that the formed GFPuv–microbead conjugate still contained the intact LPETG sorting motif (see Figure 1) and was therefore prone to subsequent SrtA-catalyzed hydrolytic and intermolecular cross-linking reactions at the LPETG sequence.[29] In general, the maximum level of fluorescence intensity of the microbead population obtained with the C-terminally His-tagged SrtA triple, tetra, and penta mutants of $SrtA_{\Delta 59}$-H_6 was at least 2- to 3-fold lower than the one obtained with the N-terminally His-tagged standard enzyme H_6-$SrtA_{\Delta 59}$ (Table 1). This indicates that despite the enhanced reaction rates observed with the SrtA mutants ^{4}*$SrtA_{\Delta 59}$-H_6 and ^{5}*$SrtA_{\Delta 59}$-H_6, the variant H_6-$SrtA_{\Delta 59}$ represents the more promising catalyst for use in immobilization reactions aiming at high protein loading of the carrier material.

CONCLUSIONS

In the present study, we investigated the use of RT-FCM for the continuous monitoring of a heterogeneous enzymatic model reaction between two entirely distinct types of substrates, i.e., a soluble target protein that is covalently coupled to a solid acceptor surface. Besides the particular SrtA-catalyzed reaction followed herein, the RT-FCM technique has practical potential for the real-time analysis of various dynamic—enzymatic and nonenzymatic—reactions directly on microparticle surfaces. To conclude our report, we summarize the unique benefits of RT-FCM for the qualitative assessment of heterogeneous dynamic reactions, and concomitantly discuss certain intrinsic requirements that may restrict the universal applicability of RT-FCM.

dx.doi.org/10.1021/bc500230r | Bioconjugate Chem. 2014, 25, 1492–1500

First of all, it should be pointed out that monitoring of molecular reactions on particles by RT-FCM relies on the use of fluorescent or fluorescently labeled substrates that (i) change the fluorescence properties of the target surface during the monitored reaction and (ii) can be excited by the laser source of the flow cytometer. The range of suitable molecules is by no means restricted to fluorescent proteins (as presented in this example), but essentially comprises all kinds of soluble synthetic and natural fluorescent molecules. Thus, it appears obvious that RT-FCM is broadly applicable for fundamental studies of diverse dynamic enzymatic and nonenzymatic reactions at the solid−liquid interface involving intrinsically fluorescent or fluorescence-labeled biomolecules (e.g., proteins, peptides, or DNA probes) as well as synthetic fluorescent compounds.

To be suited for RT-FCM analysis, homogeneously distributed microparticles of a diameter complying with the measurable size range of the flow cytometer (usually between 1 and 50 μm) should be chosen. Except for this morphological restriction, RT-FCM is not bound to particles featuring particular material compositions or surface chemistries, provided that they are sufficiently stable in aqueous suspension over the reaction period. This facilitates the use of RT-FCM for comparative studies on the suitability of different types of microparticles for, e.g., synthetic reactions.

In contrast to end point measurements, in which the properties of the immobilized product after completion of the coupling reaction are evaluated, RT-FCM provides the opportunity to detect the generation of the immobilized fluorescent product directly at the particle surface in a continuous manner without the need for individual sampling steps. The constant uptake of suspended microparticles through the fluidic system of the flow cytometer enables real-time monitoring of the progressing reaction until the sample solution in the reaction vessel is consumed or the upper detection limit of the instrument is reached (one million particle events per experiment in the case of the Accuri C6 flow cytometer). Due to the large number of continuously recorded data points, influences of reaction parameters such as temperature, pH, and salt conditions as well as sudden effects of particular test compounds can be conveniently and immediately assessed in a qualitative manner while the reaction of interest proceeds.

If the above-mentioned criteria can be satisfied, we consider RT-FCM a promising technique that facilitates the straightforward investigation of dynamic reactions occurring on particles sized in the low micrometer range. With regard to protein immobilization on solid materials, we further suggest the use of RT-FCM (i) to qualitatively compare the kinetics of the SrtA-catalyzed reaction with other enzymatic and chemical covalent immobilization strategies[8,9] and (ii) to optimize reaction parameters of the conjugation procedures for enhanced immobilization performance. Moreover, we are convinced that RT-FCM can easily be adapted for monitoring and improving other types of heterogeneous enzymatic reaction systems, such as the SrtA-catalyzed labeling of biomarkers on living cells[55,56] and liposomes.[17]

EXPERIMENTAL PROCEDURES

Production of SrtA Variants and GFPuv Target Proteins. All SrtA variants (H_6-SrtA$_{\Delta 59}$, H_6-SrtA$_{\Delta 59}$, SrtA$_{\Delta 59}$-H_6, ^{3}*SrtA$_{\Delta 59}$-H_6, ^{4}*SrtA$_{\Delta 59}$-H_6, and ^{5}*SrtA$_{\Delta 59}$-H_6; see Table 1) and GFPuv target proteins (GFPuv-linker-LPETGG-H_6 and GFPuv-linker-LAETGG-H_6)[46,57] used in this study were expressed in *E. coli* strains and purified by immobilized metal affinity chromatography as described previously.[29]

Triglycine Functionalization of Alkyl-Amino Polystyrene Microbeads. Polybead amino-terminated microspheres (mean diameter 3 μm; 1.68 × 10^9 beads per mL) were purchased from Polysciences Inc. (Warrington, PA, USA) and functionalized with a triglycine peptide linker according to a protocol adapted from a previously published report.[16] Initially, 100 μL of the bead suspension was washed three times with 500 μL of 100 mM 2-(*N*-morpholino)ethanesulfonic acid (MES) buffer (pH 4.8) by spinning in 500 μL centrifugal filter devices (0.45 μm; VWR International GmbH, Dietikon, Switzerland). After resuspending the beads in 200 μL of MES buffer in glass vials, Fmoc-Gly_3-OH (Bachem AG, Bubendorf, Switzerland) was added to a final concentration of 0.8 mM from a 100 mM stock solution dissolved in dimethylformamide (DMF). The conjugation reaction was initiated by the addition of 1-ethyl-3-(3-(dimethylamino)propyl)carbodiimide hydrochloride (EDC; Sigma-Aldrich, Buchs, Switzerland) to a final concentration of 8 mM from a 100 mM stock solution, and the suspension was shaken at room temperature for 2 h. The chemical reaction was terminated by transferring the beads to a fresh spin tube and washing the microbeads twice with 500 μL MES buffer and twice with 500 μL filtered deionized H_2O (mqH_2O) by centrifugation. Subsequently, the beads were resuspended in 200 μL of mqH_2O, transferred to a fresh glass vial, and the deprotection reaction of the Fmoc-protected peptide coupled to the microbeads was initiated by the addition of 20% (v/v) piperidine (Sigma-Aldrich). After 20 min the suspension was once more transferred to a fresh centrifugal filter device and washed twice with 500 μL of mqH_2O and twice with 500 μL of 50 mM Tris-HCl pH 7.8, 150 mM NaCl, 0.1% (v/v) Tween 20. The washed microbeads were eventually resuspended in the initial volume (100 μL) of 50 mM Tris-HCl pH 7.8, 150 mM NaCl, 0.1% (v/v) Tween 20, and stored at 4 °C until used for flow cytometry measurements.

Description of the RT-FCM Method. The major steps of the standard protocol developed for RT-FCM analysis of SrtA-catalyzed GFPuv immobilization on polystyrene microbeads are described in the first part of the Results section. Here, we define the device-specific parameters and settings of the employed Accuri C6 flow cytometer (BD Biosciences, San Jose, CA, USA) and further elaborate on the individual measurement steps (see also Figure 2).

All RT-FCM experiments were routinely performed at room temperature (25−26 °C) and without stirring of the suspensions, as only negligible bead sedimentation was observed over the monitored reaction period. Samples were run at a preset fow rate of 14 μL/min, and a primary trigger value was set on particle size using a forward scatter (FSC) threshold of 10 000; the latter setting ensured that only events of a size larger than this cutoff value were detected, thus preventing overflow of the software with noise signals caused by, e.g., instrument background, GFPuv molecules, or small-sized protein aggregates. Particles were excited with a 488 nm solid-state laser. Scattered light signals were acquired at angles of 0° ± 13° (FSC) and 90° ± 13° (SSC), and the emitted fluorescence was detected at a wavelength of 533 nm.

As depicted in Figure 2, the enzymatic reactions monitored by RT-FCM involved three sequential additions of reactants in open 1.5 mL Eppendorf polypropylene tubes. Before each addition, data acquisition was briefly paused until the reaction

suspension was supplemented and briefly mixed by careful vortexing. In general, 10 μL of a 1:20 diluted stock suspension of triglycine-functionalized polystyrene microbeads were initially added to 990 μL of reaction buffer (50 mM Tris-HCl buffer pH 7.8, 150 mM NaCl, 10 mM $CaCl_2$), yielding a suspension of approximately 0.9 × 10^6 beads per mL. The microbead suspension was processed by RT-FCM for 2 min. Subsequently, 1 μL of a 500 μM stock solution of GFPuv-linker-LPETGG-H_6 was added to the reaction mixture to yield a final target protein concentration of 0.5 μM. The suspension was monitored for another 2 min before the enzymatic reaction was initiated by addition of the desired SrtA variant to a final concentration of 2 μM (4 μL of a 500 μM stock solution). The SrtA-catalyzed immobilization reaction was followed for 56 min by RT-FCM and the obtained sets of raw data were analyzed as described in the Results section and in Figure 2. Depending on the composition of the reaction mixtures, the rate of total events counted by the flow cytometer ranged between 1000 and 1500 events per μL of liquid.

Analysis of GFPuv-Microbead Conjugates by Fluorescence Microscopy. Approximately 10^7 alkyl-amino terminated or triglycine-functionalized microbeads were suspended in a total volume of 200 μL, containing 20 μM GFPuv-linker-LPETGG-H_6 and 10 μM H_6-$SrtA_{\Delta 59}$ in 50 mM Tris-HCl buffer (pH 7.8), 150 mM NaCl, 10 mM $CaCl_2$. The reaction suspensions were incubated in 2 mL Eppendorf tubes at a temperature of 37 °C under vigorous shaking (750 rpm) using an Eppendorf Thermomixer comfort (Vaudaux-Eppendorf AG, Schönenbuch, Switzerland). After 3 h the enzymatic reactions were stopped by centrifuging the suspensions and washing the harvested microbeads twice with 500 μL of 50 mM Tris-HCl pH 7.8, 150 mM NaCl, 0.1% (v/v) Tween 20. Eventually, the beads were resuspended in a final volume of 100 μL of buffer and analyzed with a Leica DM6000B microscope equipped with a DFC350 FX monochrome digital camera (Leica Microsystems AG, Heerbrugg, Switzerland). Settings used for the acquisition of fluorescence images were kept constant in order to ensure the comparability of the bead fluorescence intensities among the respective images.

AUTHOR INFORMATION

Corresponding Author

*E-mail: michael.richter@empa.ch. Phone: +41 58 765 7868. Fax: +41 58 765 7499.

Notes

The authors declare no competing financial interest.

ACKNOWLEDGMENTS

We thank Hansueli Weilenmann for constant technical assistance with the RT-FCM system at Eawag and Prof. Harald F. Krug from the Department "Materials meet Life" at Empa for supporting the master thesis and follow-up project of PHP.

REFERENCES

(1) Sheldon, R. A., and van Pelt, S. (2013) Enzyme immobilisation in biocatalysis: why, what and how. *Chem. Soc. Rev. 42*, 6223−6235.

(2) Clouthier, C. M., and Pelletier, J. N. (2012) Expanding the organic toolbox: a guide to integrating biocatalysis in synthesis. *Chem. Soc. Rev. 41*, 1585−1605.

(3) DiCosimo, R., McAuliffe, J., Poulose, A. J., and Bohlmann, G. (2013) Industrial use of immobilized enzymes. *Chem. Soc. Rev. 42*, 6437−6474.

(4) Ispas, C. R., Crivat, G., and Andreescu, S. (2012) Review: recent developments in enzyme-based biosensors for biomedical analysis. *Anal. Lett. 45*, 168−186.

(5) Gruhl, F. J., Rapp, B. E., and Lange, K. (2013) Biosensors for diagnostic applications. *Adv. Biochem. Eng. Biotechnol. 133*, 115−148.

(6) Amine, A., Mohammadi, H., Bourais, I., and Palleschi, G. (2006) Enzyme inhibition-based biosensors for food safety and environmental monitoring. *Biosens. Bioelectron. 21*, 1405−1423.

(7) Liu, S., Zheng, Z., and Li, X. (2013) Advances in pesticide biosensors: current status, challenges, and future perspectives. *Anal. Bioanal. Chem. 405*, 63−90.

(8) Wong, L. S., Khan, F., and Micklefield, J. (2009) Selective covalent protein immobilization: strategies and applications. *Chem. Rev. 109*, 4025−4053.

(9) Redeker, E. S., Ta, D. T., Cortens, D., Billen, B., Guedens, W. J., and Adriaensens, P. (2013) Protein engineering for directed immobilization. *Bioconjugate Chem. 24*, 1761−1777.

(10) Benešová, E., and Králová, B. (2012) Affinity interactions as a tool for protein immobilization, in *Affinity Chromatography* (Magdeldin, S., Ed.) pp 29−46, InTech.

(11) Algar, W. R., Prasuhn, D. E., Stewart, M. H., Jennings, T. L., Blanco-Canosa, J. B., Dawson, P. E., and Medintz, I. L. (2011) The controlled display of biomolecules on nanoparticles: a challenge suited to bioorthogonal chemistry. *Bioconjugate Chem. 22*, 825−858.

(12) Tanaka, Y., Tsuruda, Y., Nishi, M., Kamiya, N., and Goto, M. (2007) Exploring enzymatic catalysis at a solid surface: a case study with transglutaminase-mediated protein immobilization. *Org. Biomol. Chem. 5*, 1764−1770.

(13) Wong, L. S., Thirlway, J., and Micklefield, J. (2008) Direct site-selective covalent protein immobilization catalyzed by a phosphopantetheinyl transferase. *J. Am. Chem. Soc. 130*, 12456−12464.

(14) Popp, M. W.-L., and Ploegh, H. L. (2011) Making and breaking peptide bonds: protein engineering using sortase. *Angew. Chem., Int. Ed. 50*, 5024−5032.

(15) Chan, L., Cross, H. F., She, J. K., Cavalli, G., Martins, H. F. P., and Neylon, C. (2007) Covalent attachment of proteins to solid supports and surfaces via sortase-mediated ligation. *PLoS One 2*, e1164.

(16) Parthasarathy, R., Subramanian, S., and Boder, E. T. (2007) Sortase A as a novel molecular "stapler" for sequence-specific protein conjugation. *Bioconjugate Chem. 18*, 469−476.

(17) Guo, X., Wu, Z., and Guo, Z. (2012) New method for site-specific modification of liposomes with proteins using sortase A-mediated transpeptidation. *Bioconjugate Chem. 23*, 650−655.

(18) Wu, S., and Proft, T. (2010) The use of sortase-mediated ligation for the immobilisation of bacterial adhesins onto fluorescence-labelled microspheres: a novel approach to analyse bacterial adhesion to host cells. *Biotechnol. Lett. 32*, 1713−1718.

(19) Ito, T., Sadamoto, R., Naruchi, K., Togame, H., Takemoto, H., Kondo, H., and Nishimura, S.-I. (2010) Highly oriented recombinant glycosyltransferases: site-specific immobilization of unstable membrane proteins by using *Staphylococcus aureus* sortase A. *Biochemistry 49*, 2604−2614.

(20) Leung, M. K., Hagemeyer, C. E., Johnston, A. P. R., Gonzales, C., Kamphuis, M. M. J., Ardipradja, K., Such, G. K., Peter, K., and Caruso, F. (2012) Bio-click chemistry: enzymatic functionalization of PEGylated capsules for targeting applications. *Angew. Chem., Int. Ed. 51*, 7132−7136.

(21) Clow, F., Fraser, J. D., and Proft, T. (2008) Immobilization of proteins to biacore sensor chips using *Staphylococcus aureus* sortase A. *Biotechnol. Lett. 30*, 1603−1607.

(22) Jiang, R., Weingart, J. J., Zhang, H., Ma, Y., and Sun, X.-L. (2012) End-point immobilization of recombinant thrombomodulin via sortase-mediated ligation. *Bioconjugate Chem. 23*, 643−649.

(23) Dixon, M. C. (2008) Quartz crystal microbalance with dissipation monitoring: enabling real-time characterization of biological materials and their interactions. *J. Biomol. Technol. 19*, 151−158.

(24) Sha, X., Sun, C., Xu, X., Alexander, L., Loll, P. J., and Penn, L. S. (2012) Quartz crystal microbalance (QCM): useful for developing procedures for immobilization of proteins on solid surfaces. *Anal. Chem. 84*, 10298−10305.
(25) Song, H. Y., Zhou, X., Hobley, J., and Su, X. D. (2012) Comparative study of random and oriented antibody immobilization as measured by dual polarization interferometry and surface plasmon resonance spectroscopy. *Langmuir 28*, 997−1004.
(26) Fischer, M., Leech, A. P., and Hubbard, R. E. (2011) Comparative assessment of different histidine-tags for immobilization of protein onto surface plasmon resonance sensorchips. *Anal. Chem. 83*, 1800−1807.
(27) Popp, M. W.-L., Antos, J. M., and Ploegh, H. L. (2009) Unit 15.3. Site-specific protein labeling via sortase-mediated transpeptidation. *Curr. Protoc. Protein Sci.* Published online April 1, 2009, DOI: 10.1002/0471140864.ps1503s56.
(28) Ilangovan, U., Ton-That, H., Iwahara, J., Schneewind, O., and Clubb, R. T. (2001) Structure of sortase, the transpeptidase that anchors proteins to the cell wall of *Staphylococcus aureus*. *Proc. Natl. Acad. Sci. U.S.A. 98*, 6056−6061.
(29) Heck, T., Pham, P.-H., Yerlikaya, A., Richter, M., and Thöny-Meyer, L. (2014) Sortase A catalyzed reaction pathways: a comparative study with six SrtA variants. *Catal. Sci. Technol.*, DOI: 10.1039/c4cy00347k.
(30) Martin, J. C., and Swartzendruber, D. E. (1980) Time: a new parameter for kinetic measurements in flow cytometry. *Science 207*, 199−201.
(31) Nolan, J. P., and Sklar, L. A. (1998) The emergence of flow cytometry for sensitive, real-time measurements of molecular interactions. *Nat. Biotechnol. 16*, 633−638.
(32) Shapiro, H. M. (2003) *Practical flow cytometry*, 4th ed., Wiley-Liss, Hoboken, NJ.
(33) do Céu Monteiro, M., Sansonetty, F., Goncalves, M. J., and O'Connor, J.-E. (1999) Flow cytometric kinetic assay of calcium mobilization in whole blood platelets using Fluo-3 and CD41. *Cytometry 35*, 302−310.
(34) Vines, A., McBean, G. J., and Blanco-Fernández, A. (2010) A flow-cytometric method for continuous measurement of intracellular Ca^{2+} concentration. *Cytom. Part A 77*, 1091−1097.
(35) Arnoldini, M., Heck, T., Blanco-Fernández, A., and Hammes, F. (2013) Monitoring of dynamic microbiological processes using real-time flow cytometry. *PLoS One 8*, e80117.
(36) Buranda, T., Jones, G. M., Nolan, J. P., Keij, J., Lopez, G. P., and Sklar, L. A. (1999) Ligand receptor dynamics at streptavidin-coated particle surfaces: a flow cytometric and spectrofluorimetric study. *J. Phys. Chem. B 103*, 3399−3410.
(37) Buranda, T., Lopez, G. P., Simons, P., Pastuszyn, A., and Sklar, L. A. (2001) Detection of epitope-tagged proteins in flow cytometry: fluorescence resonance energy transfer-based assays on beads with femtomole resolution. *Anal. Biochem. 298*, 151−162.
(38) Nolan, J. P., Shen, B., Park, M. S., and Sklar, L. A. (1996) Kinetic analysis of human flap endonuclease-1 by flow cytometry. *Biochemistry 35*, 11668−11676.
(39) Schwartz, S. L., Tessema, M., Buranda, T., Pylypenko, O., Rak, A., Simons, P. C., Surviladze, Z., Sklar, L. A., and Wandinger-Ness, A. (2008) Flow cytometry for real-time measurement of guanine nucleotide binding and exchange by Ras-like GTPases. *Anal. Biochem. 381*, 258−266.
(40) Hammes, F., and Egli, T. (2010) Cytometric methods for measuring bacteria in water: advantages, pitfalls and applications. *Anal. Bioanal. Chem. 397*, 1083−1095.
(41) Díaz, M., Herrero, M., García, L. A., and Quirós, C. (2010) Application of flow cytometry to industrial microbial bioprocesses. *Biochem. Eng. J. 48*, 385−407.
(42) Sklar, L. A. (2005) *Flow cytometry for biotechnology*, Oxford University Press, New York.
(43) Ton-That, H., Mazmanian, S. K., Faull, K. F., and Schneewind, O. (2000) Anchoring of surface proteins to the cell wall of *Staphylococcus aureus*. Sortase catalyzed in vitro transpeptidation reaction using LPXTG peptide and NH_2-Gly_3 substrates. *J. Biol. Chem. 275*, 9876−9881.
(44) Hirakawa, H., Ishikawa, S., and Nagamune, T. (2012) Design of Ca^{2+}-independent *Staphylococcus aureus* sortase A mutants. *Biotechnol. Bioeng. 109*, 2955−2961.
(45) Ton-That, H., Mazmanian, S. K., Alksne, L., and Schneewind, O. (2002) Anchoring of surface proteins to the cell wall of *Staphylococcus aureus*. Cysteine 184 and histidine 120 of sortase form a thiolate-imidazolium ion pair for catalysis. *J. Biol. Chem. 277*, 7447−7452.
(46) Chen, I., Dorr, B. M., and Liu, D. R. (2011) A general strategy for the evolution of bond-forming enzymes using yeast display. *Proc. Natl. Acad. Sci. U.S.A. 108*, 11399−11404.
(47) Kruger, R. G., Dostal, P., and McCafferty, D. G. (2004) Development of a high-performance liquid chromatography assay and revision of kinetic parameters for the *Staphylococcus aureus* sortase transpeptidase SrtA. *Anal. Biochem. 326*, 42−48.
(48) Kruger, R. G., Otvos, B., Frankel, B. A., Bentley, M., Dostal, P., and McCafferty, D. G. (2004) Analysis of the substrate specificity of the *Staphylococcus aureus* sortase transpeptidase SrtA. *Biochemistry 43*, 1541−1551.
(49) Möhlmann, S., Mahlert, C., Greven, S., Scholz, P., and Harrenga, A. (2011) *In vitro* sortagging of an antibody Fab fragment: overcoming unproductive side reactions of sortase with water and lysine chains. *ChemBioChem 12*, 1774−1780.
(50) Schwartz, A., Wang, L., Early, E., Gaigalas, A., Zhang, Y.-Z., Marti, G. E., and Vogt, R. F. (2002) Quantitating fluorescence intensity from fluorophore: the definition of MESF assignment. *J. Res. Natl. Inst. Stand. Technol. 107*, 83−91.
(51) Wang, L. L., Gaigalas, A. K., Abbasi, F., Marti, G. E., Vogt, R. F., and Schwartz, A. (2002) Quantitating fluorescence intensity from fluorophores: Practical use of MESF values. *J. Res. Natl. Inst. Stand. Technol. 107*, 339−353.
(52) Wu, Y., Campos, S. K., Lopez, G. P., Ozbun, M. A., Sklar, L. A., and Buranda, T. (2007) The development of quantum dot calibration beads and quantitative multicolor bioassays in flow cytometry and microscopy. *Anal. Biochem. 364*, 180−192.
(53) Anne, A., and Demaille, C. (2012) Kinetics of enzyme action on surface-attached substrates: a practical guide to progress curve analysis in any kinetic situation. *Langmuir 28*, 14665−14671.
(54) Halling, P. J., Ulijn, R. V., and Flitsch, S. L. (2005) Understanding enzyme action on immobilised substrates. *Curr. Opin. Biotechnol. 16*, 385−392.
(55) Tanaka, T., Yamamoto, T., Tsukiji, S., and Nagamune, T. (2008) Site-specific protein modification on living cells catalyzed by sortase. *ChemBioChem 9*, 802−807.
(56) Yamamoto, T., and Nagamune, T. (2009) Expansion of the sortase-mediated labeling method for site-specific N-terminal labeling of cell surface proteins on living cells. *Chem. Commun. 9*, 1022−1024.
(57) Duong, A., Capstick, D. S., Di Berardo, C., Findlay, K. C., Hesketh, A., Hong, H.-J., and Elliot, M. A. (2012) Aerial development in *Streptomyces coelicolor* requires sortase activity. *Mol. Microbiol. 83*, 992−1005.